Urethane-forming reaction kinetics and catalysis of model palm olein polyols: Quantified impact of primary and secondary hydroxyls

Tuan Noor Maznee Tuan Ismail,[1] Kosheela Devi Poo Palam,[1] Zailan Bin Abu Bakar,[1] Hoong Seng Soi,[1] Yeong Shoot Kian,[1] Hazimah Abu Hassan,[1] Christi Schiffman,[2] Aisa Sendijarevic,[2] Vahid Sendijarevic,[2] Ibrahim Sendijarevic[2]

[1]Synthesis and Product Development Unit, Advanced Oleochemical Technology Division, Malaysian Palm Oil Board Kajang, Selangor, Malaysia

[2]Troy Polymers, Inc., Troy, Michigan, 48083

Correspondence to: I. Sendijarevic (E-mail: sendijarevic@troypolymers.com)

ABSTRACT: Model palm olein natural oil polyols (NOPs) with varying ratios of primary to secondary hydroxyls were synthesized, characterized, and evaluated in reaction kinetics study with isocyanate in formation of polyurethanes. Reaction rate constants and activation energies associated with primary and secondary hydroxyls of NOPs were quantified. The kinetic study in toluene shows that the NOP containing primary hydroxyls have three times higher reaction rate constants in noncatalyzed reaction with 4,4'-diphenylmethane diisocyanate (4,4'-MDI) compared to the model NOP containing only secondary hydroxyls, which is associated with higher activation energy of secondary hydroxyls. However, the difference in reaction rate constants of primary and secondary hydroxyls in NOPs diminished in the reactions catalyzed with dibutyltin dilaurate. Bulk polymerization reaction confirms the kinetics results in toluene, showing that the model NOP containing primary hydroxyls reached gel time at a faster rate. Evaluation of elastomers from bulk polymerization shows low degree of phase separation of hard and soft segments for elastomers based on the model NOPs. © 2015 Wiley Periodicals, Inc. J. Appl. Polym. Sci. **2016**, *133*, 42955.

INTRODUCTION

Polyurethanes are one of the most diversified types of polymers in terms of the application diversity and can be found as solid coatings, elastomers, adhesives, sealants, flexible foams, and rigid foams. To meet the specific requirements of each application, numerous raw materials have been developed for the syntheses of polyurethanes, including a variety of isocyanates and polyols which are the two key components for the syntheses of polyurethanes.[1–5]

Isocyanates used in the polyurethanes have either aromatic or aliphatic backbone and are petroleum-based monomers with functionality of two or higher.[1–5] Polyols are multifunctional oligomers with hydroxyl groups that react with isocyanates to form polyurethanes.[1–5]

Polyether polyols constitute the largest volume of the polyol used in polyurethanes.[5] Polyether polyols are produced via addition polymerization of the initiators with propylene oxide and/or ethylene oxide, which are derived from petroleum sources.[1–4] Polyester polyols are also used in significant quantities in production of polyurethanes, and are produced via reactions of

multifunctional alcohols with diacids, which can include adipic acid, phthalic acid (or phthalic anhydride), and caprolactones, which for most part are petroleum based products.[1–5]

To reduce the dependence on the petroleum-based raw materials and improve the sustainability and availability of polyurethane products, new classes of polyester polyols have been under development based on renewable raw materials.[6–13] To produce natural oil polyols (NOPs) with high renewable content, various chemical paths have been developed to convert alkenes in the aliphatic backbone of triglycerides to hydroxyls.[10–13] Natural oils evaluated for the syntheses of polyols include vegetable, animal, and algae oils, which can be commonly characterized as triglycerides with varying degrees of unsaturation in the aliphatic backbone. Syntheses of NOPs most commonly entails epoxidizing of the alkenes in oils with *in situ* generated peroxy acids, and subsequently opening of the epoxides into hydroxyls via various synthetic routes.[10–13]

In rigid and flexible polyurethane foam applications, NOPs have been used in conjunction with the conventional polyether and

polyester polyols, and typically constitute low percentages of the final polyurethane product.[14] Amid various backbone differences between conventional polyether polyols and NOPs, a difference in reactivities between the two classes of polyols has been attributed as one of the reasons for low introduction of NOPs in polyurethanes. In comparison to the conventional polyether and polyester polyols which are terminal, the reactivity of NOPs with isocyanates is typically lower due to a hindered location of pendant hydroxyl groups in the aliphatic backbone of the triglyceride molecule.[15] The hindered location of pendant hydroxyls in the aliphatic backbone of NOPs can also impact physical properties of the resulting polyurethanes.[14–20]

Depending on the chemical process used for opening of the epoxides into hydroxyls, NOPs can be produced with varying ratios of primary and secondary hydroxyls.[11–20] For conventional polyether polyols, it is well known that primary hydroxyls are more reactive than the secondary hydroxyls. As an example, polyether polyols produced from propylene oxide, which yield terminal secondary hydroxyls, are typically three times less reactive with isocyanate than the analogue polyols which are ethoxylated at the end of the polymerization reaction to yield terminal primary hydroxyls.[1–4] Numerous studies have reported the impact of primary versus secondary hydroxyl groups on the kinetics and catalysis of reaction of polyether polyols with isocyanates; however, these correlations have not been systematically evaluated for reactivity of NOPs with isocyanates.[1–4, 21,22]

It has been reported that the NOP with higher primary hydroxyl content was more reactive in polyurethane-forming reaction than the NOP with all secondary hydroxyls.[20] Guo et al. reported that the NOP with primary hydroxyls in polymerization reaction with isocyanate reached gel time at faster rates than the NOP with all secondary hydroxyls.[19] It has also been reported that the reactivity of the NOP with secondary hydroxyls can be increased via ethoxylation of the secondary hydroxyls, which converts them into primary hydroxyls.[15] However, the determination of reaction rate constants and activation energies associated with reactivity of primary versus secondary hydroxyls in NOPs with isocyanates have not been determined in the referenced studies.

The aim of this work is to systematically evaluate and quantify the impact of the primary versus secondary hydroxyl groups on the polymerization reaction kinetics of model NOPs with 4,4′-MDI. The kinetic study was completed with model NOPs produced from epoxidized palm olein (EPOo), following the chemical routes that produced two polyols—one model polyol with a mixture of primary and secondary hydroxyls and the other model polyol with only secondary hydroxyls. To our knowledge, this is the first study that systematically evaluates the impact of primary and versus secondary hydroxyls on the reactivity of NOPs with 4,4′-MDI in a solvent, and quantifies the associated reaction rate constants, activation energies, and response to catalyst. The reactivity of the two model NOPs with isocyanates was also compared in a bulk polymerization with 4,4′-MDI at 90°C. The resulting elastomers were analyzed via differential scanning calorimetry (DSC), dynamic mechanical analyses, atomic force microscopy (AFM), and small angle X-ray scatter-

ing (SAXS) to determine the impact of the model NOPs on the phase separation of hard and soft segments.

EXPERIMENTAL

Materials

A sample of EPOo with oxirane oxygen content of 3.27% and iodine value 0.797 g I_2/100 g was provided by Malaysian Palm Oil Board (MPOB). All other materials, solvents, and reagents were purchased from commercial suppliers and unless otherwise noted were used as received.

Synthesis of Palm Olein E-135 NOP was carried out in a pilot plant consisting of a 1000 L jacketed stainless steel reactor, equipped with mechanical agitator, and thermocouple. A total of 270 kg of EPOo was placed in a reactor and preheated to 60–65°C under agitation. A freshly prepared mixture of 34.98 kg ethylene glycol (99% reagent grade ethane-1,2-diol from Kong Long Huat Chemicals) and 1.38 kg of BF_3 diethyl ether complex (50% boron trifluoride in diethyl ether from Merck Sdn Bhd) was added slowly to the preheated EPOo. The addition of ethylene glycol (EG) mixture with BF_3 diethyl ether complex was stopped every time the reaction temperature increases to 100–110°C at which point the reaction mixture was cooled until the temperature dropped to 95°C. The total addition time for the EG mixture was 80 min. The reaction mixture was prolonged for additional 50 min at 95°C until the alcoholysis was completed (oxirane oxygen content decreased to 0.03%).

Subsequently, the reaction mixture temperature was decreased to 45°C and the product was neutralized and washed using the following procedure. Three hundred kilograms of tap water preheated to 55–60°C was added to the product and the mixture was stirred for 2 min. The mixture was then allowed to separate for 30 min and aqueous fraction was decanted. The washing step was repeated with 300 kg of 3% NaCl solution, followed by 300 kg of 0.5% Na_2CO_3 solution two times, consecutively. The final wash was carried out with 300 kg water. The pH of the final product was 5. After the final wash, the final product was dried under a vacuum of 80–70 mbar and temperature of 70–75°C for 13 h. The total weight of the final product was 284.5 kg (96.0% yield based on starting EPOo). Idealized reaction schematic for syntheses of model NOP E-135 is presented in Figure 1.

Synthesis of Palm Olein M-60 NOP was carried out using a 10 L laboratory water jacketed glass reactor equipped with a condenser, thermocouple, addition funnel, and mechanical agitator. The heating and cooling was provided with a water circulated bath. A total of 3.0 kg of EPOo was placed in the reactor and preheated to 50–55°C under agitation. A BF_3/methanol mixture, which was prepared by adding 15 g of boron trifluoride diethyl ether complex (50% BF_3 in diethyl ether) to 190.5 g of methanol (99.8% methyl alcohol from Friendemann Schmidt), was added slowly to the preheated EPOo. The addition of BF_3/methanol mixture was stopped every time when the reaction temperature increased to 60°C at which point the reaction mixture was cooled to 50–55°C. After the addition of BF_3/methanol mixture was completed, mixing was continued for additional 35 min maintaining the reaction temperature at 50–55°C. At that
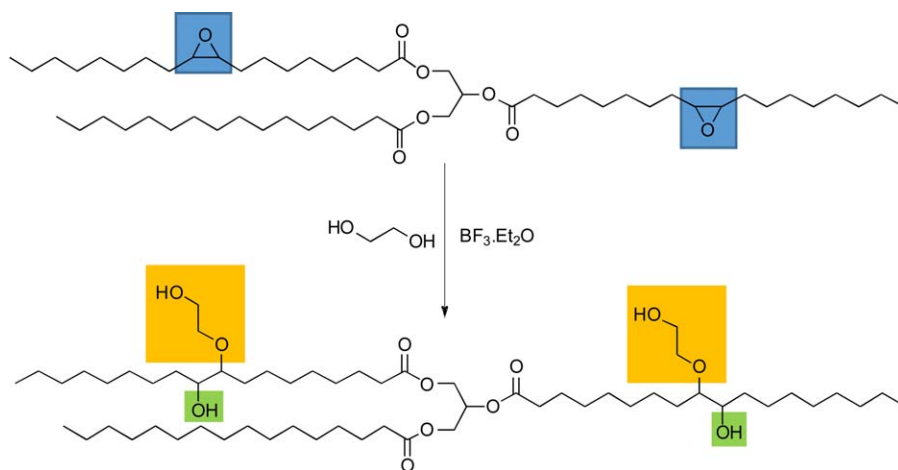
Figure 1. Idealized schematic of ring opening of epoxidized palm olein with ethylene glycol for synthesis of a model NOP E-135 with primary and secondary hydroxyl groups. [Color figure can be viewed in the online issue, which is available at wileyonlinelibrary.com.]

point, the alcoholysis was completed (oxirane oxygen content decreased to 0.03%).

Afterwards, the product was neutralized and washed at 60–65°C using the following procedure. The heating was provided by the water circulated bath attached to the 10 L water jacketed glass reactor. The product was washed with 4 kg of 1% NaCl solution, followed by 4 kg of 0.5% Na_2CO_3 solution until the pH of the product was about 6–8, which was measured using pH paper. The final wash was with 1% NaCl solution in order to remove the residual carbonate solution. The pH of the final washed product was 6–7. The neutralized polyol product was dried under vacuum of 17 mmHg at 85–100°C until the moisture content reached 0.1%. The total weight of the final product was 2.75 kg (88.70% yield based on starting EPOo). Idealized reaction schematic for syntheses of model NOP M-60 is presented in Figure 2.

Polyol Analyses Methods
Hydroxyl value (ASTM D4274-05), acid value (ASTM D4662-08), iodine value (AOCS Cd 1d-92), oxirane oxygen content (AOCS Cd 9-57), and moisture content (ASTM D4672-00) in polyols

were determined according to the respective methods. Moisture content was measured on Coulometric Karl Fischer Titrator, Model 275KF, Titration Controller Model 260 (Denver Instrument). Fourier transfer infrared (FTIR) spectra were recorded on a Perkin Elmer Spectrum Two with Pike Miracle ATR Attachment. Viscosities of polyols were measured using a Brookfield Viscometer, Model LVF. Thermal properties were determined via differential scanning calorimetry (DSC Q 10, TA Instruments) at a heating rate of 10°C/min under nitrogen sweep.

Molecular weight distributions were determined using a gel permeation chromatograph (GPC) consisting of a Waters 515 HPLC Pump, Auto sampler (SIL-20A/20AC, Shimadzu), Waters 2410 Differential Refractometer (Waters, Milford, MA), On-line Degasser, Model JMDG-4 (JM Science, Grand Island, NY), a set of four Phenogel 5 μm (300 $\times$ 7.8 mm) 50 Å; 10^2 Å, 10^3 Å, and 10^4 Å GPC columns (all Phenomenex, Torrance, CA) covering a MW range of $10^2 - 10^6$, and a Guard column: 5 μm linear/mixed, 50 $\times$ 7.8 mm. The flow rate of tetrahydrofuran eluent was 1 mL/min. The columns and detector were thermostated at 40°C.
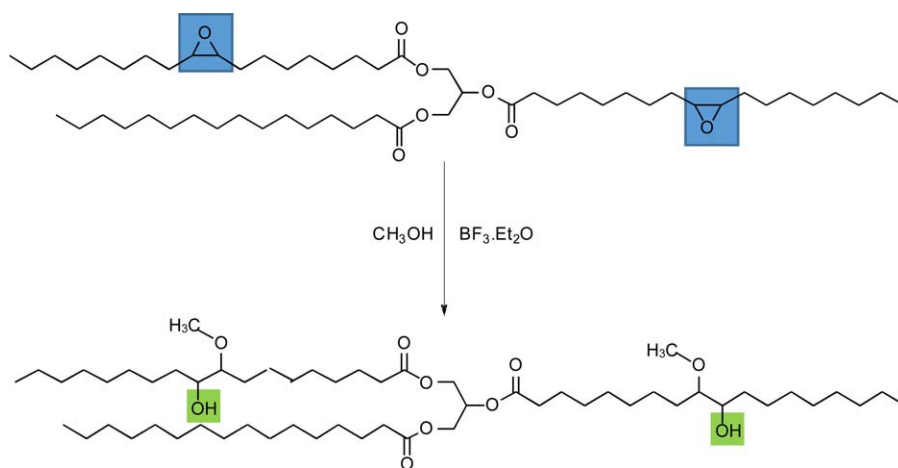

Figure 2. Idealized schematic of ring opening of epoxidized palm olein with methanol for synthesis of a model NOP M-60 with secondary hydroxyl groups. [Color figure can be viewed in the online issue, which is available at wileyonlinelibrary.com.]
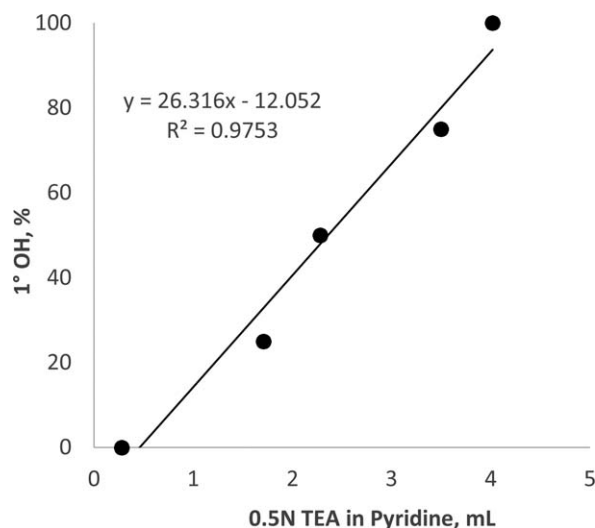
Figure 3. Calibration graph for determination of primary and secondary hydroxyl groups generated using *sec*-butanol and isobutyl alcohol at 100/0, 75/25, 50/50, 25/75, and 0/100 ratios.

The content of primary to secondary hydroxyl groups in polyols was analyzed using a titration method following a protocol described by Fijolka.[23] Polyols were dried under vacuum of ≤ 2.5 mm Hg at 70°C until the moisture was $\leq 0.03\%$. A vial containing 2.5 mmol of polyol based on hydroxyl groups, 5.4 mmol (1.5 g) of chlorotriphenylmethane (98% from Alfa Aesar), and 15 mL of pyridine ($\geq 99\%$ from Chempure) was placed in an oven at 50°C for 2 h. The vial was shaken at 10, 30, 60, and 90 min. After 2 h, the vial was removed and cooled to room temperature. The walls of the vial were rinsed with 30 mL of dried acetone ($\geq 99.5\%$ from Sigma-Aldrich) and then the solution titrated to a neutral endpoint (pH 7.0) with 0.5N triethylamine (TEA) ($\geq 99\%$ TEA from Sigma-Aldrich) in pyridine using a 1 mL glass pipet graduated to 0.01 mL. The endpoint was determined potentiometrically with a pH meter (Extech Instruments Oyster-10 pH/mV/Temperature meter with pH electrode model 60120B). The same protocol was followed for a blank solution consisting of 5.4 mmol (1.5 g) chlorotriphenylmethane, and 15 mL pyridine. pH of the final solution was 7.0 and thus the amount of the titrant was 0 mL. For the determination of primary and secondary hydroxyl contents, a standard calibration graph was constructed using 25/75, 50/50 and 75/25 blends by equivalents of isobutyl alcohol (spectrometric grade from Mallinckrodt with 100% primary hydroxyl content) to 2-butanol (99% from Sigma with 100% secondary hydroxyls) (Figure 3). Acetone, pyridine, isobutyl alcohol and sec-butanol used in a protocol for determination of primary and secondary hydroxyls were dried with Molecular Sieves Type Z, Grade 3A-12 (Sphinx Adsorbents).

Kinetic Measurements

The reaction of palm olein polyols M-60 and E-135 with 4,4′-MDI (Mondur M 4,4′-diphenylmethane diisocyanate, flaked from Bayer) was carried out in toluene (99.7% HPLC grade from Chem Pure Brand Chemicals) at 0.1N concentration (based on 4,4′-MDI NCO-equivalents and polyol hydroxyl equivalents) in a 1 L jacketed three-necked reaction flask equipped with nitrogen

inlet, a reflux condenser, and a thermometer. The reaction flask was connected to a Julabo MA-6 Heated Circulator with diethylene glycol as heating/cooling media. The reflux condenser was connected to Kaake K20DC3 Refrigerating Circulator with diethylene glycol as heating/cooling media thermo-stated to 7°C. A U-shaped drying absorption tube field with Molecular Sieves Type Z, Grade 3A-12 was attached to the reflux condenser to isolate the reaction mixture from the ambient moisture. Agitation was provided via electromagnetic stirrer.

4,4′-MDI was used as received from the supplier. Palm olein polyols M-60 and E-135 were dried at 70°C under vacuum of ≤ 1 mmHg until the moisture content was $\leq 0.03\%$. Toluene was dried with Molecular Sieves Type Z, Grade 3A-12. The reaction of 4,4′-MDI with palm olein polyols was carried out at 1 : 1 equivalent ratio according to the following procedure. First, 500 mL toluene was placed into the reaction flask and heated to a desired reaction temperature. Afterwards, 6.27 g of 4,4′-MDI (0.05 NCO-equivalents) was added to the toluene. The solution of 4,4′-MDI in toluene was agitated for 10 min before addition of 0.05 equivalents of a polyol (36.1 g of M-60 or 21.0 g of E-135). A time of addition of polyol was used as a starting time of the reaction. At designated times during the reaction, samples were drawn from the reaction mixture and quenched in a pre-weighed solution of di-n-butyl amine ($\geq 99.5\%$ from Aldrich) in toluene for the NCO % titration in accordance with ASTM D-2572. The weight of the reaction sample was calculated from the total weight of the quenched sample and the weight of di-n-butyl amine solution used for quenching. Results of the NCO % titrations at different temperatures are shown in Table III. The impact of catalyst on reactivity was completed by adding 0.005 wt % dibutyltin dilaurate catalyst (Dabco T-12 from Air Products) with polyol to 4,4′-MDI in toluene using the same procedure as outlined in the previous paragraph.

The reactivity of model palm olein polyols with 4,4′-MDI was measured in bulk polymerization at 1.05 : 1.00 equivalent ratios with and without Dabco T-12 catalyst at 90°C by measuring gel time according to ASTM D2471-99, where gel time is defined as the time of string formation. About 22.84 g of E-135 polyol was weighed in a 100 mL polypropylene cup suited for a multi-axial mixer (Speed Mixer, DAC 400 FV, FlackTek). The cup was closed with a lid and placed in an air-circulation oven heated at 90°C. Using a 12 mL air-tight syringe (Luer Lock NORM-JECET[R] Henke SASS Wolf), 7.16 g of 4,4′-MDI conditioned at 40°C was weighed and placed in an air circulating oven at 90°C for 30 min. Afterwards, 7.16 g of isocyanate from the syringe was added to the polyol, the cup was closed and the components were mixed in the multiaxial mixer for 30 s at 2200 rpm. Immediately after mixing, the cup was placed in the oven at 90°C. The string formation was checked periodically with a spatula. Between each insertion of the spatula in the reaction mixture, the cup was closed and returned to the oven. The gel time (string formation) was calculated from a minimum of two measurements.

In the case of catalyzed reaction, 0.0012 g of Dabco T-12 catalyst was added to 22.84 g of E-135 and mixed via speed mixer for 3 min at 2200 rpm. Following procedure described for the noncatalyzed reaction, 7.16 g of isocyanate was reacted with
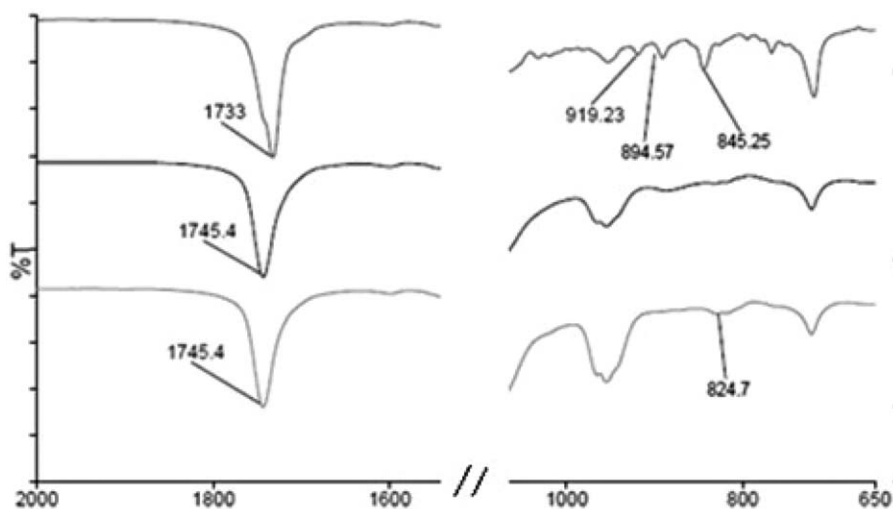
Figure 4. FTIR of epoxidized palm olein (top), E-135 polyol (middle), and M-60 polyol (bottom).

22.84 g of E-135 containing the catalyst at 90°C and time of string formation was measured. The same procedure as described above was used for gel time determination in reaction of 4,4′-MDI (4.61 g) with M-60 polyol (25.39 g), with and without Dabco T-12 catalyst (0.0012 g).

Elastomer Preparation and Analyses

Following the procedure of bulk polymerization, model NOPs and isocyanates with 0.004 wt % Dabco T-12 catalyst were mixed and at the gel time (as determined in bulk-polymerization study) the resin was poured into a pre-heated Teflon mold, and placed into a press at 90°C and about 2000 psi of pressure for 24 h. After 7 days of room temperature aging, the elastomers were confirmed to be fully cured by determining absence of isocyanate with FTIR and tested for thermal properties with DSC at 10°C/min heating rate and dynamic mechanical analyzer (Perkin Elmer, DMA 7e) at 3°C/min heating rate in bending mode. The elastomers were analyzed in a tapping mode with Atomic Force Microscope (Digital Instruments, Dimension 3100) in order to obtain the phase images. The resulting phase images were shown on 25 degree scale. SAXS was completed on Rigaku SmartLab X-ray diffractometer operating at 1.5418 Å wavelength.

RESULTS AND DISCUSSION

Syntheses and Characterization of Model NOPs

Most commercially available NOPs for polyurethanes are produced from either soybean oil or palm oil following the chemical route that as the first step entails epoxidizing of unsaturated natural oils. For this study, we used EPOo. Methods for epoxidizing of natural oils, including palm olein, were described in the following references.[24–26]

Two model NOP polyols were produced from EPOo with different ratios of primary and secondary hydroxyls. As shown in Figure 1, EPOo was reacted with EG to form a model NOP E-135 with a mixture of primary and secondary hydroxyls. Figure 2 shows the reaction of EPOo with methanol, which results in formation of a model NOP M-60 with one secondary hydroxyl per epoxide.

FTIR spectra in Figure 4 show that the reactions of EPOo with EG and methanol resulted in complete conversions of epoxides into hydroxyls, as evident by the lack of signal at 845 cm^{-1} in E-135 and M-60 associated with epoxides.[27] Using a titration method per AOCS Cd 9-57 it was also confirmed that E-135 and M-60 polyols have oxirane oxygen content of 0.03% compared to 3.27% of the starting EPOo (Table I).

Concentration of hydroxyl groups, reported as hydroxyl value, in E-135 is almost double that of M-60, which is expected as the ring opening with EG yields two hydroxyls per epoxide versus one hydroxyl generated from ring opening of epoxide with methanol (Figures 1 and 2). Conversely, the equivalent weight (calculated from hydroxyl value) is higher for M-60 than E-135.[4]

The GPC data in Figure 5 show an increase in molecular weight in M-60 and E-135 polyols compared to starting EPOo

Table I. Properties of Palm Olein Polyols M-60 and E-135 and Starting EPOo

Designation	M-60	E-135	EPOo
Hydroxyl value, mg KOH/g	77.64	133.98	–
Acid value, mg KOH/g	0.66	0.70	0.69
Moisture content, %	0.17	0.15	0.09
Oxirane oxygen content, %	0.03	0.03	3.27
Iodine value, g I$_2$/100 g	8.40	7.02	0.80
Viscosity at 25°C, Cp	2,000	4,400	–
T_m, °C	13.29	14.75	–
GPC data	1995	2175	910
Mn, Daltons	4125	5530	980
Mw, Daltons	2.07	2.54	1.08
Mw/Mn			
Equivalent weight (Eq. Wt.)[a]	722.57	420.60	–
Hydroxyl functionality[b]	2.8	5.2	–

[a] Calculated from hydroxyl value.
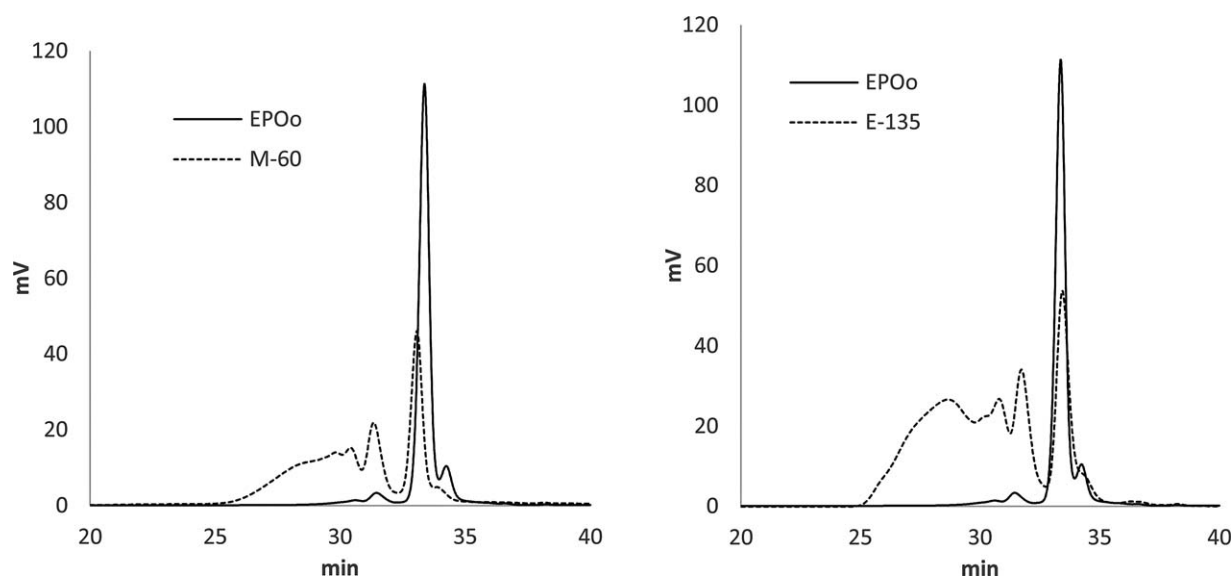[b] Ratio of Mn to Eq.Wt.

Figure 5. on left GPC chromatograms of EPOo and M-60 NOP. On right, GPC chromatograms of EPOo and E-135 NOP.

(Table I). As expected, the number average molecular weight (Mn) and weight average molecular weight (Mw) is higher for E-135 than M-60. E-135 and M-60 have significantly higher polydispersity index (PDI) than EPOo, which suggests intermolecular reactions of epoxide groups via alcoholysis. Higher PDI in E-135 suggests that primary hydroxyls participate in intermolecular bonding more readily than the secondary hydroxyls.

The average functionality, defined as the ratio of Mn from GPC measurements to equivalent weight calculated from hydroxyl value, was 5.2 for E-135 and 2.8 for M-60 (Table I). It was anticipated that the model E-135 NOP would have higher functionality than M-60 NOP as reaction of EPOo with EG yields two hydroxyl per epoxide, whereas EPOo reaction with methanol yields one hydroxyl per epoxide. However, both model NOPs have functionality greater than 2 and therefore reaction with difunctional 4,4′-MDI would result in polymerization into polyurethane.

To confirm the primary and secondary hydroxyl content, each NOP was analyzed via a titration method utilizing triphenylmethane procedure developed by Fijolka.[23] The method involves development of a titration curve based on mixtures of *sec*-butanol and *iso*butyl alcohol which contain 100% secondary hydroxyls and 100% primary hydroxyls, respectively (Figure 3). The

method was validated on poly(oxypropylene) glycol (Arcol PPG 725 polyol from Bayer), which yielded 100% secondary hydroxyl content, as expected (Table II). The method was also validated with ethoxylated glycerine (Lumulse POE 26 from Lambent Technologies) with 26 moles of ethylene oxide per one mole of glycerol, where the primary hydroxyl content was determined to be 98.5%.

For M-60 NOP, the titration yielded 94.4% secondary hydroxyls content, which is close to the theoretical value of 100% (Table II). For E-135 NOP, the titration yielded 39.5% primary hydroxyls with remaining hydroxyls being secondary (Table II). For E-135, the theoretical primary content is 50%. During the syntheses of E-135, primary hydroxyls probably participate in inter and intramolecular bonding with unreacted epoxides, reducing the primary hydroxyl content in the final polyol. DSC analyses of the two NOPs show that both have pronounced melt transitions, with melt transition temperatures for E-135 and M60 at 14.7°C and 13.3°C, respectively (Figure 6).

Polymerization Reaction Kinetics

The focus of this study was to evaluate the impact of the primary and secondary hydroxyls on the reactivity of the model NOPs with isocyanate in both uncatalyzed and tin catalyzed urethane-forming reactions. In-depth overviews of the isocyanate reactions are presented in the following reference.[1–3,28,29] The reaction between isocyanate and alcohol is an exothermic reaction and it results in formation of urethanes (Scheme 1). In order to promote the polymerization rates of polyurethanes, organotin catalysts are utilized to effectively promote the formation of urethane bonds. The mechanism for the formation of urethanes catalyzed by organotin catalysts is presented in Scheme 2.[28,29]

The urethane-forming reaction rate of model M-60 NOP and E-135 NOP with 4,4′-MDI were completed in toluene at various temperatures by following the change in NCO % from 4,4′-MDI over a 6-h period. By limiting the conversions of 4,4′-

Table II. Determination of Primary and Secondary Hydroxyl Group Concentrations via Titration

Sample	Titrant, mL[a]	1° OH, %[b]	2° OH, %[b]
E-135	1.96	39.5	60.5
M-60	0.67	5.6	94.4
POE-26	4.23	99.3	0.7
PPG-725	0.27	0	100

[a] 0.5N solution of triethylamine (TEA) in pyridine using 2.5 mmol of hydroxyl equivalent for each polyol.
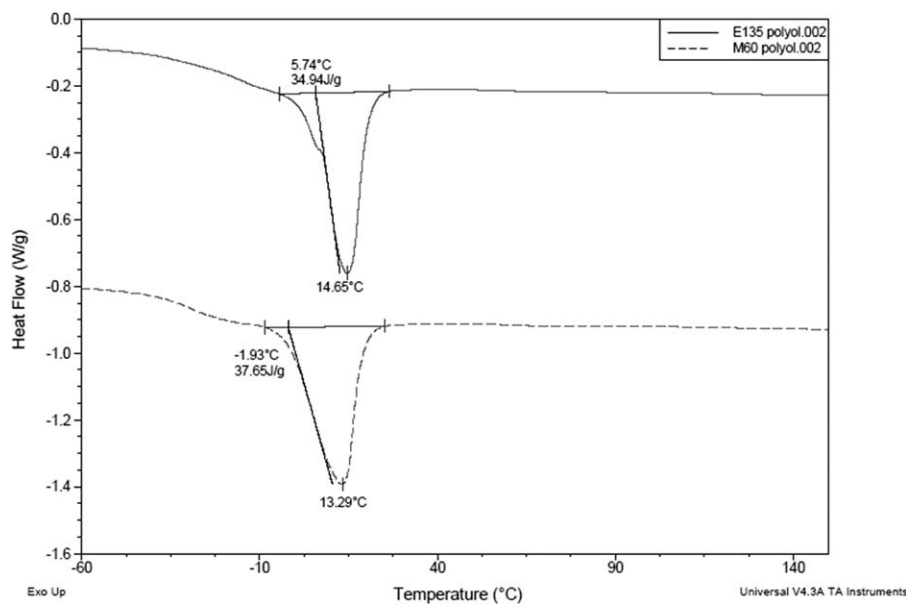[b] Calculated from calibration curve in Figure 5.

Figure 6. Thermal transitions determined with DSC on E-135 and M60 NOPs.

MDI, we were also able to isolate the impacts of primary hydroxyls on the reactivity of E-135 NOP. Also, by limiting the conversion of 4,4′-MDI, we limited the extend of polymer formation, which could introduce stearic hindrance and affect the kinetics results. As the data in Table III show, E-135 NOP reacted with 4,4′-MDI at a faster rate than M-60 NOP. These results confirm that higher concentration of primary hydroxyls in NOPs increases the reactivity of the polyols with isocyanates, despite the fact that these hydroxyls are not terminal in the polyol chain.

It is generally accepted that the simple urethane formation reaction is characterized by the second order kinetics [eq. (1A)].[1–3,28,30] In this study the starting equivalent ratio of polyols and isocyanates was equal, and, assuming negligible side isocyanate reactions, it is reasonable to assume that the equivalent

concentration of isocyanate and polyols should remain equal throughout the reaction. Therefore, the second order kinetics can be represented by eq. (1B).

$$-d[R_1NCO]/d[t] = k\,[R_2OH]\,[R_1NCO] \qquad (1A)$$

$$-d[NCO]/d[t] = k\,[R_1NCO]^2 \qquad (1B)$$

As shown in Figure 7, the model E-135 NOP with 39.5% primary hydroxyl content is significantly more reactive than model M-60 NOP with 94.4% secondary hydroxyl content in reaction with isocyanate in toluene. Also, the data in Figure 7 show that the reaction rate for both polyols fit well the second order kinetics, and second-order reaction rate constants were 2.5–3.5 times higher for E-135 NOP compared to M-60 NOP (Table IV). Due to the limited extent of the isocyanate conversion, the second-order kinetics fit for E-135 NOP reflects the reaction

Table III. Concentration of Isocyanate in Reaction of 4,4′-MDI with M-60 and E-135 Polyols in Toluene at indicated Temperatures

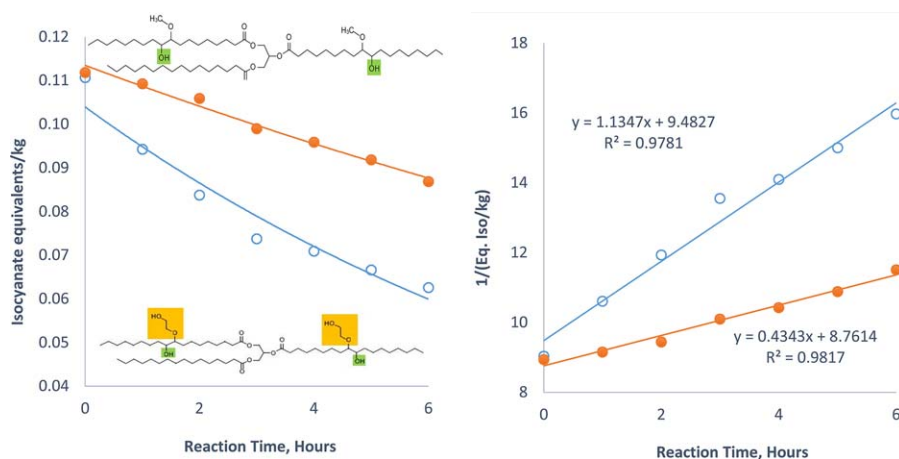| Polyol	M-60				E-135		
T (°C)	50	80	90	100	50	80	90
Reaction time, h	NCO %				NCO %		
0	0.460	0.453	0.470	0.460	0.452	0.459	0.465
0.5	0.455	0.443	–	–	0.425	0.429	–
1	0.460	0.427	0.459	–	0.399	0.407	0.396
1.5	0.454	0.421	–	0.420	0.395	0.382	–
2	0.444	0.415	0.445	–	0.392	0.345	0.352
3	0.423	0.404	0.416	0.389	0.374	0.329	0.310
4	0.404	0.390	0.403	–	0.353	0.301	0.298
4.5	–	–	–	0.376	–	–	–
5	0.412	0.386	0.386	–	0.302	0.286	0.280
6	0.415	0.380	0.365	0.354	0.291	0.270	0.263

Figure 7. Left: change in Isocyanate Equivalents with time for reaction of 4,4′-MDI with M-60 NOP (solid circles) and E-135 NOP (open circles) in toluene at 90°C. Right: second-order reaction kinetics of 4,4′-MDI with M-60 NOP (solid circles) and E-135 NOP (open circles) in toluene at 90°C. [Color figure can be viewed in the online issue, which is available at wileyonlinelibrary.com.]

kinetics associated with the primary hydroxyls. On the other hand, the reactions of isocyanate with M-60 NOP reflect the reaction kinetics of the secondary hydroxyls.

In conventional polyether polyols, the ratio of reactivity of terminal primary hydroxyls to terminal secondary hydroxyls has been reported to be about 10 : 3.[4] In a model study of phenyl isocyanate with alcohols in benzene, it was shown that among aliphatic alcohols the relative rates of reaction of primary, secondary, and tertiary alcohols are approximately 1.0, 0.3, and 0.003–0.007, respectively.[2] In toluene at 20°C, it was shown that the reaction of isocyanates with *n*-butanol had 2.3 times higher reaction rate constant compared to 2-propanol.[2] Therefore, the impact of primary and secondary pendant hydroxyls of NOPs on reactivity with isocyanates is comparable to conventional polyether polyols and alcohols, despite the fact that in polyether polyols hydroxyl groups are terminal.[1–3]

The temperature dependence of the second order reaction rate constants are plotted in Figure 8, and as the data show the reaction rate constants fit the Arrhenius dependence.

$$k = Ae^{\left(-\frac{E}{RT}\right)} \tag{3}$$

The data in Table IV show that M-60 NOP has higher activation energy in reaction with isocyanate than E-135 NOP. Therefore, these results confirm that the activation energy of NOPs in reaction with isocyanates increases with secondary hydroxyl content in NOPs. The same trend was observed in the reaction kinetics study of butanol with 4,4′-MDI, where higher activation energy was determined for the isocyanate reactions with sec-butanol than *n*-butanol.[28]

The impact of dibutyl tin dilaurate catalyst was also evaluated on the reactivity of M-60 NOP and E-135 NOP with isocyanate in toluene at 50°C (Figure 9). In general, organotin compounds are known to be effective catalysts in polyurethane reactions and it has been reported that dibutyl tin dilaurate catalyst at 0.1% concentration increases the reaction rate constant 210 times compared to uncatalyzed system.[28] The kinetic study completed in toluene demonstrate that the discrepancy in reactivities between primary and secondary hydroxyls diminished in response to the addition of 0.005 wt % dibutyltin dilaurate catalyst. For M-60 NOP with higher content of secondary hydroxyls, the addition of catalyst resulted in 6.8 times increased reaction rate constants compared to 2.6 times increase with E-135 NOP. These results suggest that dibutyl tin dilaurate

Table IV. Second-Order Reaction Rate Constants for Reaction of 4,4′-MDI with Palm Olein Polyols M-60 and E-135 in Toluene at Different Temperatures

Olyol	M-60			E-135		
T (°C)	Equation	R^2	k ([NCO]h)$^{-1}$	Equation	R^2	k ([NCO]h)$^{-1}$
50	$y = 0.227x + 9.3$	0.822	0.227	$y = 0.810x + 9.3$	0.946	0.810
50[a]	$y = 1.544x + 10.4$	0.984	1.544	$y = 2.084x + 11.8$	0.882	2.084
80	$y = 0.293x + 9.4$	0.961	0.293	$y = 1.073x + 9.4$	0.983	1.073
90	$y = 0.434x + 8.8$	0.981	0.434	$y = 1.134x + 9.5$	0.978	1.134
100	$y = 0.442x + 9.3$	0.983	0.442	–	–	–
Arrhenius relationship	Ea 3.340 kcal/mol			Ea 2.003 kcal/mol		

[a] Reaction completed in the presence of Dabco T12 catalyst. Equations follow the same format as in Figure 7, where *y* represents an inverse of isocyanate equivalents/kg and *x* represents reaction time in hours.
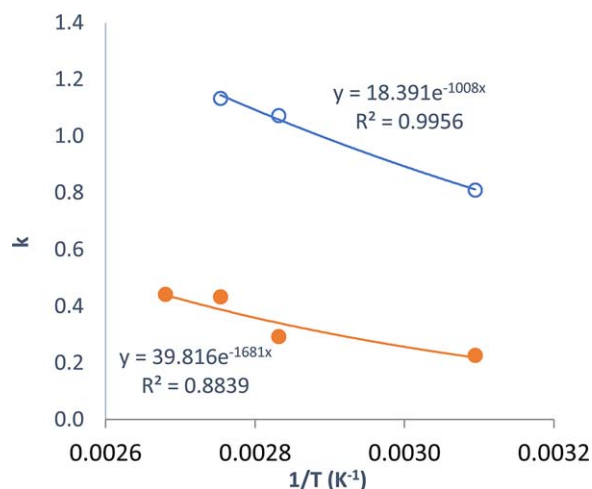
Figure 8. Arrhenius plot for second-order reaction constants of 4,4′-MDI with palm olein polyols M-60 (solid circles) and E-135 (open circles) in toluene. [Color figure can be viewed in the online issue, which is available at wileyonlinelibrary.com.]

catalyst effectively overcomes the higher activation energy associated with the presence of secondary hydroxyls in NOPs.

The results of reaction kinetics of two model NOPs with isocyanates in toluene are expected to translate to the polyurethane applications, which for most part involve bulk polymerization. For this reason, the two model NOPs were reacted with 4,4′-MDI in bulk. The reactivity of the two model NOPs with 4,4′-MDI was completed at 1.00 : 1.05 equivalent ratios with and without dibutyltin dilaurate (Dabco T12) catalyst at 90°C. The polymerization reaction rate was captured by the measurement of gel time according to ASTM D2471-99, where gel time is defined as the time of string formation.

As data in Table V show, M-60 NOP in noncatalyzed polymerization reaction with 4,4′-MDI at 90°C reached gel time at 51.9 min, whereas E-135 NOP reached gel time at 6.0 min. In polymerization reactions between the NOPs with isocyanates catalyzed with 0.004 wt % Dabco T12 catalyst, gel times of 26.0 min and 2.6 min were recorded for reaction of M-60 NOP

Table V. Gel Time in Minutes for Bulk Polymerization of 4,4′-MDI with Palm Olein Polyols M-60 and E-135 at 90°C[a]

Sample	No catalyst	0.004% Catalyst[b]
E-135	6.0 ± 0.0	2.6 ± 0.2
M-60	51.9 ± 2.7	26.0 ± 1.4

[a] Gel time determined according to ASTM D2471-99.
[b] Dabco T12 catalyst.

and E-135 NOP, respectively. Therefore, the addition of catalysts approximately doubled the reaction rates of both NOPs with isocyanate in the bulk polymerization.

In both catalyzed and non-catalyzed bulk polymerizations, E-135 NOP with 39.5% primary hydroxyl content reached gel time at 8–10 times faster rate than M-60 NOP, which virtually contained only secondary hydroxyls. For comparison, in toluene the second-order reaction rate constants for E-135 were 2.5–3.5 times higher than those of M-60. The discrepancy in the rate of gelling in the bulk polymerization versus reaction rate constant in toluene could be explained by the fact that gel time in bulk polymerization does not only depend on the reactivity of the components but is also impacted by other factors that can include the functionality of the polyols and intramolecular and intermolecular bonding.[31–34]

Elastomer Analyses

It is expected that in addition to their impact on reactivity, varying ratio of primary to secondary hydroxyls in NOPs could impact the thermo-mechanicals properties of polyurethanes and potentially the formation of hard and soft segment domains. The fully cured elastomers produced via bulk polymerization of 4,4′-MDI with E-135 NOP and M-60 NOP were analyzed via DMA. As shown in Figure 10, in glassy state both samples have comparable plateau G' values of about 6×10^9 Pa and in rubbery state the plateau value of G' appears significantly higher for the elastomer based on E-135 NOP with higher content of primary hydroxyls and higher functionality. Broader tangent delta curve for elastomer based on E-135 NOP could correlate with a reduction in soft and hard segment separation. The DSC
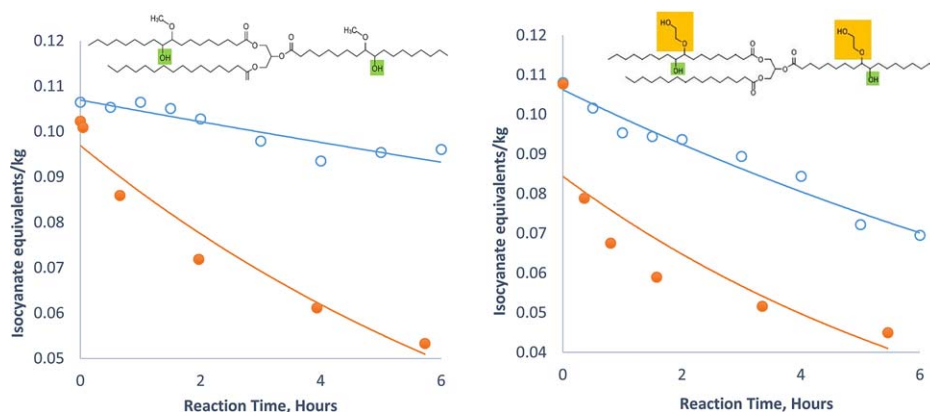

Figure 9. Change is isocyanate equivalents in reaction of 4,4′-MDI with palm olein polyol M-60 (left graph) and E-135 (right graph) with Dabco T-12 catalysts (solid circles) and without T-12 catalyst (open circles) in toluene at 50°C. [Color figure can be viewed in the online issue, which is available at wileyonlinelibrary.com.]
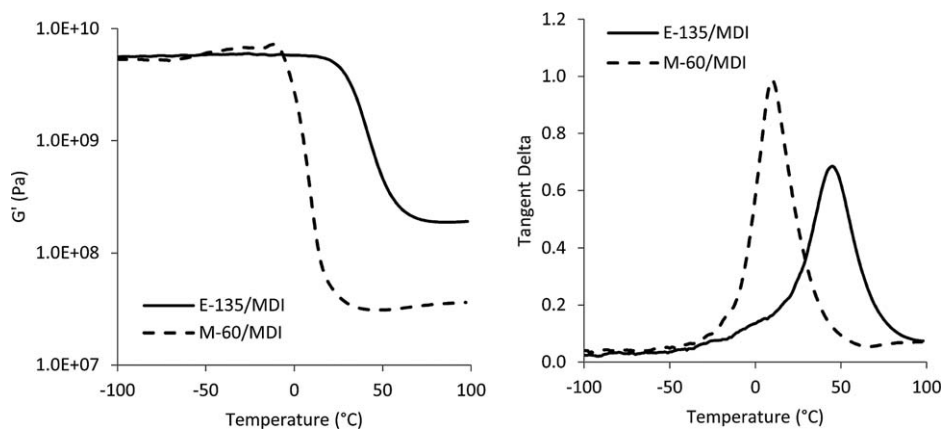
Figure 10. DMA results of fully cured elastomers produced via bulk polymerization of 4,4'-MDI with E-135 NOP and M-60 NOP polyether polyols.
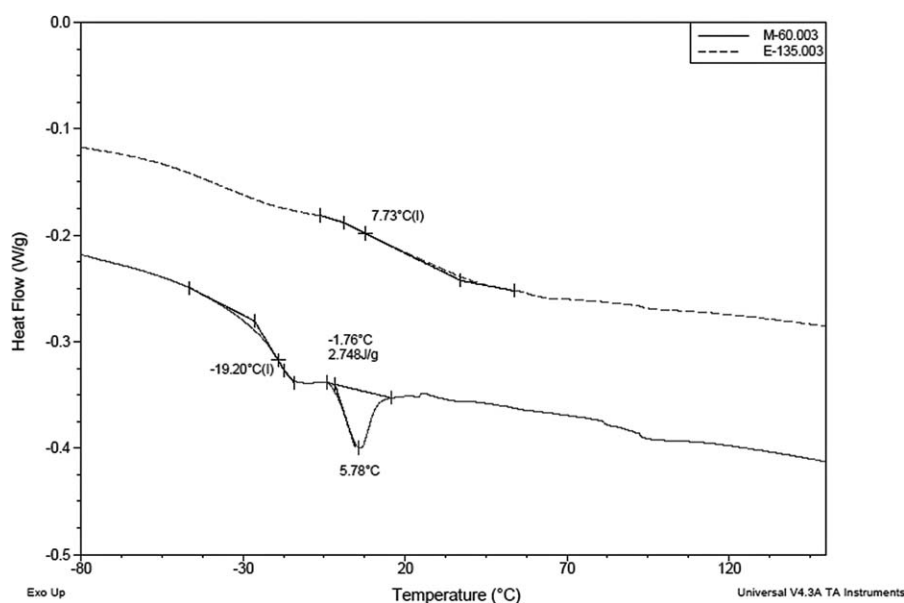

Figure 11. DSC analyses of the fully cured elastomers produced via bulk polymerization of 4,4′-MDI with E-135 NOP and M-60 NOP polyether polyols.

analyses of the elastomers (Figure 11) show that the elastomer based on E-135 NOP has no melt transition while the polyol itself does (Figure 6), which further indicates that E-135 NOP's soft segment is well mixed with the hard segment. On the other hand, the DSC analyses of the elastomer based on M-60 polyol shows a melt transition at 5.8°C, which, while significantly
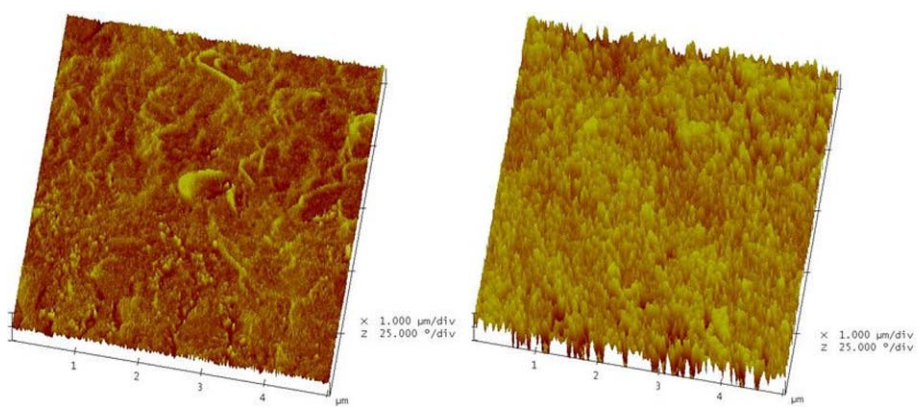
Figure 12. AFM phase images on the fully cured elastomers produced via bulk polymerization of 4,4′-MDI with M-60 NOP (left) and E-135 NOP (right). [Color figure can be viewed in the online issue, which is available at wileyonlinelibrary.com.]
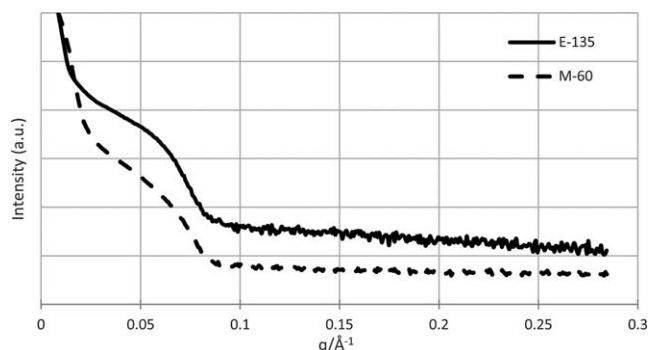
Figure 13. SAXS profiles of the fully cured elastomers produced via bulk polymerization of 4,4′-MDI with M-60 NOP and E-135 NOP.

attenuated, is most likely associated with the polyol (Figure 6). Therefore, the data suggests that the increased functionality of the NOP contributed to an increased mixing of the soft and hard segments.

Phase images of the elastomers collected via AFM are presented in Figure 12. The images were collected via tapping mode, and hard domains are represented by lighter colors and softer matrix by darker colors.[35,36] The elastomer based on M-60 NOP is composed of the small structures agglomerated into lamella like larger domains. The elastomer made from E-135 NOP does not contain lamella structure, but it does have discrete domains which appear to be cylindrical and uniformly distributed on the surface. SAXS analyses of the elastomers are presented in Figure 13. The SAXS data for both elastomers show no scattering maxima, indicating lack of scattering domains. However, both materials show a diffused shoulder like peak at 0.05 Å^{-1} corresponding to the inter-domain spacing of 12.6 nanometers. This result compares well to the reported interdomain separation of scattering domains in polyurethane foams; however, the scattering intensity in this study is very low.[35,36] This is most likely due to the fact that the NOPs in this study act like cross-linkers in polyurethane elastomers, which adds to the mixing of the soft and hard segment domains.

CONCLUSIONS

Model palm olein-based NOPs with varying ratio of primary to secondary hydroxyls were synthesized, characterized, and evaluated in reaction kinetics study with isocyanate in formation of polyurethanes. Reaction rate constants and activation energies associated with primary and secondary hydroxyls of NOPs were quantified. The kinetic study completed in toluene demonstrates that the model NOP which contained primary hydroxyls had on average about three times higher second-order reaction rate constant than the NOP with mostly secondary hydroxyls, which correlates well with the impact of terminal primary and secondary hydroxyls on reactivity of petroleum-based polyether polyols. The results show that the changes in reactivity of NOPs with isocyanates can be attributed to increased activation energy associated with secondary hydroxyls. However, it was demonstrated that dibutyl tin dilaurate catalyst effectively overcomes the higher activation energy associated with the secondary
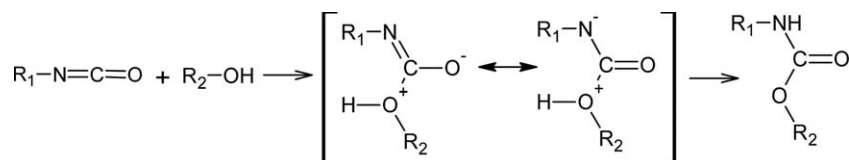
Scheme 1. Noncatalyzed urethane formation mechanism via isocyanate reaction with polyol.
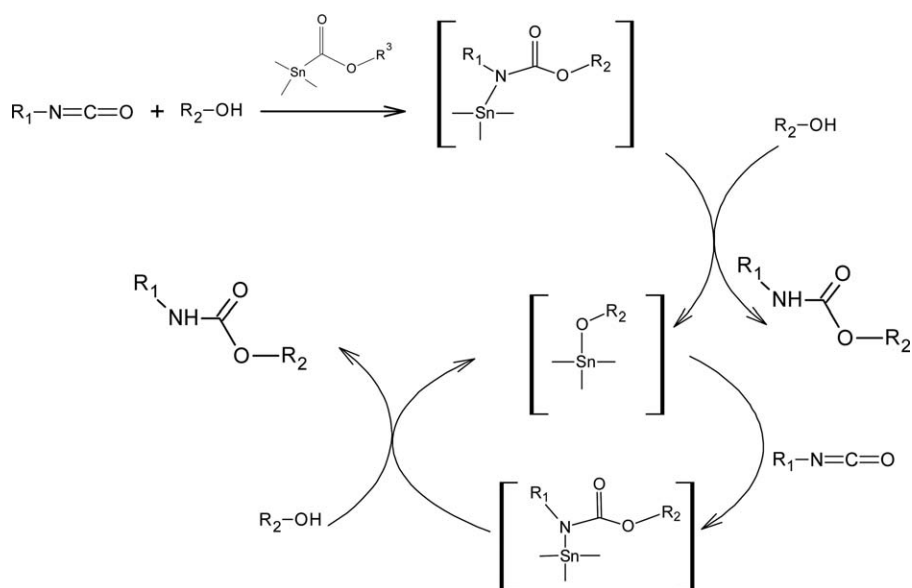
Scheme 2. Organotin catalyzed urethane formation via isocyanate reaction with polyol.[28]

hydroxyls in NOPs. Results of bulk polymerization of the model NOPs with 4,4′-MDI also confirm that the polyol with higher primary hydroxyl content reached gel time faster, and the impact of catalyst was comparable for both polyols. This study provides a quantifiable impact of primary and secondary pendant hydroxyls on the reaction kinetics and catalysis of NOPs, which can be used to guide more systematic incorporation of NOPs in polyurethane applications. The results also show that in the elastomer based on the model NOPs, there exists very little separation of hard and soft segment domains.

ACKNOWLEDGMENTS

REFERENCES

1. Oertel, G. Polyurethane Handbook; Hanser: Munich, **1985**.

2. Saunders, J. H.; Kurt, C. F. Polyurethanes: Chemistry and Technology; Interscience Publisher: New York, **1962**.

3. Ionescu, M. Chemistry and Technology of Polyols for Polyurethanes; Rapra Technology Limited: Shawbury, **2005**.

4. Herrington, R.; Hock, K. Flexible Polyurethane Foams; Dow Chemical Company: **1997**.

5. 2014 End-Use Market Survey for Polyurethanes Industry in the United States, Canada and Mexico; American Chemistry Council: Washington, **2015**.

6. Miller, R.; Janssen, R. Theunissen. L. Proceeding of the 2012 CPI Polyurethanes Technical Conference, Atlanta, Georgia, 24–26 September **2012**.

7. Coggio, W. D. Proceeding of the 2014 CPI Polyurethanes Technical Conference, Dallas, Texas, 22–22 September **2014**.

8. Theunissen, L.; Janssen, R. Proceeding of the 2014 CPI Polyurethanes Technical Conference, Dallas, Texas, 22–22 September **2014**.

9. Mang, M. N. Proceeding of the 2013 CPI Polyurethanes Technical Conference, Phoenix, Arizona, 23– 25 September **2013**.

10. Hill, K. *Pure Appl. Chem.* **2000**, *72*, 1255.

11. Petrović, Z. S. *Contemp. Mater.* **2010**, *I-1*, 39.

12. Desroches, M.; Escouvois, M.; Auvergne, R.; Caillol, S.; Boutevin, B. *Polym. Rev.* **2012**, *52*, 38.

13. Petrović, Z. S. *Polym. Rev.* **2008**, *48*, 109.

14. Sendijarevic, V. *International Palm Oil Congress - Oleochemical and Specialty Chemicals Conference.* **2011**, 59.

15. Ionescu, M.; Petrović, Z. S.; Wan, X. *J. Polym. Environ.* **2007**, *15*, 237.

16. Pawlik, H.; Prociak, A. *J Polym. Environ.* **2012**, *29*, 438.

17. Tan, S.; Abraham, T.; Ference, D.; Macosko, C. W. *Polymer* **2011**, *52*, 2840.

18. John, J.; Bhattacharya, M.; Turner, R. B. *J. Appl. Polym. Sci.* **2002**, *86*, 3097.

19. Guo, A.; Zhang, W.; Petrović, Z. S. *J. Mater. Sci.* **2006**, *41*, 4914.

20. Campanella, A.; Bonnaillie, L. M.; Wool, R. P. *J. Appl. Polym. Sci.* **2009**, *112*, 2567.

21. Volkova, E. R.; Tereshatov, V. V.; Karmanov, V. I. *J. Appl. Spectrosc.* **2010**, *77*, 737.

22. Lovering, E. G.; Laidler, J. L. *Can. J. Chem.* **1962**, *40*, 31.

23. Fijolka, P. *PlasteKautsch.* **1971**, *18*, 431.

24. Saurabh, T.; Patnaik, M.; Bhagt, S. L.; Renge, V. C. *Ijaet* **2011**, *II*, 491.

25. Derawi, D.; Salimon, J. *J. Chem.* **2010**, *7*, 1440.

26. Abu Hassan, H.; Tuan Ismail, T. N. M.; Sattar, M. N.; Hoong, S. S.; Ooi, T. L.; Ahmad, S.; Poo Palam, K. D.; Cheong, M. Y. US 7932409 B2, **2011**.

27. González, M. G.; Cabanelas, J. C.; Baselga, J. Infrared Spectroscopy—Materials Science, Engineering and Technology; Theophanides, T. Eds.; InTech Publising: **2012**, Chapter 13, p 265.

28. Delebecq, E.; Pascault, J.; Boutevin, B.; Ganachaud, F. *Chem. Rev.* **2012**, *113*, 80.

29. Sardon, H.; Pascual, A.; Mecerreyes, D.; Taton, D.; Cramail, H.; Hedrick, J. L. *Macromolecules* **2015**, *48*, 3153.

30. Nagy, T.; Antal, B.; Czifrak, K.; Papp, I.; Karger-Kocsis, J.; Zsuga, M.; Keki, S. *J. Appl. Polym. Sci.* **2015**, *132*, 42127.

31. Luo, Q.; Liu, M.; Xu, Y. F.; Ionescu, M.; Petrović, Z. S. *Macromolecules* **2011**, *44*, 7149.

32. Lu, Y.; Larock, R. C. *Biomacromolecules* **2008**, *9*, 3332.

33. Flory, P. J. *J. Am. Chem. Soc.* **1941**, *63*, 3083.

34. Matejka, L.; Dusek, K. *Polym. Bull.* **1980**, *3*, 489.

35. Sharma, C.; Kuma, S.; Unni, R. A.; Aswal, V. K.; Rath, S. K.; Harikrishnan, G. *J. Appl. Polym. Sci.* **2014**, *131*, 40668.

36. Zhang, L.; Jeon, H. K.; Malsam, J.; Herrington, R.; Macosko, C. W. *Polymer* **2007**, *48*, 6656.